METHODS

Patient 1

Patient 1 is an 18-month-old girl who initially presented with hydrops fetalis and mild facial dysmorphism (mild frontal bossing, hypertelorism, and depressed nasal bridge) and later had failure to thrive, hepatosplenomegaly with transaminitis, chronic cytopenias, arthralgias, nodular rashes, and recurrent febrile episodes. Her anemia was transfusion dependent, and her baseline platelet count was approximately $30 \times 10^3/\mu L$. Both cytopenias were nonautoimmune in nature but secondary to hypersplenism. Her parents were not related.

Further laboratory evaluation revealed a massive increase in CRP levels (55 mg/L), ESR (>130 mm/h), and ferritin levels (2364 ng/mL). She had normal levels of plasma soluble IL-2 receptor (soluble CD25). Serum levels of IL-6 and IL-18, as well as IL-18BP, were significantly increased (Table I). Immunophenotypic changes in monocytes and natural killer cells (Fig 1, *A* and *B*) were also noted. Because of the complex nature of the disease, WES was performed and identified a heterozygous and possibly pathogenic *de novo* variant in *CDC42* c.563G>A (p.C188Y; Fig 1).

Therapy with the IL-1 receptor antagonist anakinra was initiated, and within 48 hours, the patient experienced an increase in appetite and improved mobility. Over the course of the following weeks, fever, anemia, thrombocytopenia, and rash entirely resolved; the spleen massively decreased in size; and the patient started to meet developmental milestones. CRP levels and ESR normalized over a period of 6 months, whereas ferritin and free IL-18 levels continue to trend downward (Fig 1, *D*, and Table I). Increases in monocyte phosphoprotein levels also normalized after 4 months of treatment (Fig 1, *D*).

Patient 2

Patient 2 is a 22-month-old girl who presented in the neonatal period with dysmorphic features (frontal bossing, macrocephaly, thin sparse hair, and depressed nasal bridge), respiratory distress, and cholestasis with transaminitis requiring intensive care. Subsequently, she had recurrent febrile episodes associated with respiratory symptoms and macular skin lesions. In addition to failure to thrive, her physical examination showed generalized lymphadenopathy and hepatosplenomegaly. Infectious history was positive for 2 episodes of otitis media with perforation of the tympanic membrane and 1 episode of severe bronchiolitis with enterovirus. The latter required invasive ventilation. Laboratory evaluation revealed thrombocytopenia with a baseline platelet count of $35 \times 10^3/\mu L$ and transfusion-dependent anemia. There was no history of consanguinity.

Further investigations demonstrated increased CRP (56 mg/L), ferritin (875 μg/L), and lactate dehydrogenase (LDH; 540 ng/L) levels. She had an increased soluble IL-2 receptor level (sCD25; 8657 U/mL [normal range, 278-1580 U/mL]; Table I).

With concern for MAS, therapy with anakinra was initiated and titrated to a dose of 6 mg/kg. This led to a dramatic improvement in inflammatory markers and resolution of fevers. WES was performed and identified a monoallelic and possibly pathogenic *de novo* mutation in *CDC42* c.563G>A (p.C188Y). Twelve months after initiation of treatment with anakinra, the patient had significantly improved growth parameters and started to meet developmental milestones. Her cytopenias and rashes resolved, and transaminitis and splenomegaly improved (Fig 1, *D*, and Table I). She continues with subclinical inflammation and mildly increased CRP and serum ferritin levels. Through her disease course, she had 2 episodes of suspected viral gastroenteritis. Her clinical course was also complicated by multiple respiratory tract infections with negative viral study results, except for one that had a positive respiratory culture to human metapneumovirus.

Patient 3

Patient 3 is a now 6.5-year-old white girl who presented at birth with purpuric rash, grade II brain hemorrhage, hepatosplenomegaly, thrombocytopenia (approximately $25 \times 10^3/\mu L$), and leukocytosis. She also rapidly had macular rashes, frequent febrile episodes, and chronic cytopenias (anemia, thrombocytopenia, and neutropenia). Her anemia and thrombocytopenia were transfusion dependent. Her parents were not related. Further laboratory evaluation revealed an increased CRP level of 142 mg/L, an ESR of 62 mm/h, hyperferritinemia (5191 μg/L), and increased LDH levels (817 ng/L, Table I).

She responded poorly to prednisone, immunoglobulin replacement therapy, and rituximab. At the age of 5 months, she was started on anakinra (3 mg/kg) with improvement of the rash and fever. Anakinra dose was progressively increased to 8.5 mg/kg, resulting in improvement but not complete resolution of anemia, thrombocytopenia, hyperferritinemia, and systemic inflammation (Fig 1, *D*, and Table I). WES was performed and identified a monoallelic and possibly pathogenic *de novo* mutation in *CDC42* c.556C>T (p.R186C). She also had rare variants in *LYST* and *UNC13D* (Fig 1, *A*, and Table E2). Anakinra was stopped, and canakinumab doses were increased to eventually 8.0 mg/kg once monthly. This resulted in further improvement of the anemia, thrombocytopenia, and normalization of the WBC. The need for transfusion was dramatically decreased.

She has had recurrent episodes of anterior cervical lymphadenitis (some with abscess formation) and 1 episode of β-hemolytic strep sepsis with purpura fulminans. She has chronic hepatosplenomegaly. Growth is at the fifth percentile for height and weight. Social and intellectual development are normal.

Patient 4

Patient 4 is a now 12-year-old Hispanic boy without any family history of consanguinity who presented in the neonatal period with fever, papular erythematous rash, hepatosplenomegaly, transaminitis, and leukocytosis. Cerebrospinal fluid collected had 60 WBCs with 60% neutrophils and increased protein. He also had anemia and thrombocytopenia.

At 7 weeks of age, he presented with seizures caused by a small intracranial hemorrhage/hematoma secondary to severe thrombocytopenia. Between 2 and 8 months of life, his anemia (approximately 7.4 g/dL) and thrombocytopenia (approximately $56 \times 10^3/\mu L$) were transfusion dependent, and he still had hepatosplenomegaly, recurrent fever, rash, increased CRP level (44 mg/L on 2.5 mg/kg anakinra), ESR (140 mm/h), and LDH (322 U/L; normal range, <226 U/L) on 2.5 mg/kg anakinra. At 8 months, he was found to have retinal detachment, phthisis of his right eye and papilledema of the left eye, both of which were presumed to be secondary to his inflammatory disease and increased intracranial pressure.

Because of the patient's phenotypic similarities to patients with NOMID, he was started on prednisone and anakinra at age 8 months, with resolution of systemic inflammation and cytopenias. Before 18 months of age, while receiving 1 mg/kg/d prednisone and anakinra, he had respiratory syncytial virus–induced pneumonia, septic arthritis, and cervical lymphadenitis. The infections resolved when steroids were discontinued. His psychomotor development was mildly delayed. At age 9 years, when anakinra was switched to canakinumab, he had *Staphylococcus aureus* bacteremia and septic myositis with multiple abscesses and was switched back to anakinra with ongoing control of the systemic inflammation while completing antibiotic therapy. The patient has not presented with chronic hyperferritinemia, and the highest documented ferritin level was 470 ng/mL (normal range, <336 ng/mL) during the episode of septic myositis. WES identified a monoallelic and possibly pathogenic *de novo* variant in *CDC42* c.576A>C (stop loss; p.*192C*24).

The patient is currently 12 years old and receiving treatment with anakinra. His systemic inflammation presenting with fever, rash, anemia, and thrombocytopenia has resolved, and liver and spleen sizes have normalized (Fig 1, *D*, and Table I). His growth parameters have improved, and he grows along the 10th percentile for height and weight.

Serum cytokine measurement

Total IL-18, IL-18BP, and CXCL9 levels were measured, as described by Weiss et al.[E1]

Mass cytometry: Whole blood and antibody staining

Blood was drawn in EDTA vacutainer tubes. The samples used for experiments were fixed within 1 hour of blood draw by using Smart Tube

Proteomic Stabilizer (Smart Tube, San Carlos, Calif) and stored at −80°C. The samples were thawed in a cold room, and red cells were lysed with 1× Smart Tube Thaw-Lyse Buffer (Smart Tube). Each sample was labeled and acquired in a CyTOF machine individually. Samples were stained with an Fc receptor blocker (Human TruStain FcX; BioLegend, San Diego, Calif), followed by incubation with a cocktail of pretitrated metal-conjugated antibodies (23 antibodies, Table E1) for surface staining for 30 minutes at room temperature. Samples were then washed, fixed with 1.6% formaldehyde (Thermo Scientific, Rockford, Ill), and permeabilized with 90% ice-cold methanol overnight. Next-day samples were washed and stained with a cocktail of antibodies for intracellular protein and phosphoprotein (7 antibodies, Table E1) for 30 minutes at room temperature. After washing, the samples were incubated with 0.125 nmol/L iridium (191Ir and 193Ir; Cell-ID Intercalator-Ir; Fluidigm, South San Francisco, Calif) to enable cell identification based on DNA content and acquired on the same day.

Data acquisition and analysis

For acquisition, the samples were resuspended at a concentration of approximately 1 million cells/mL in a solution of 1:10 Calibration Beads (Calibration Beads, EQ Four ELEMENT; Fluidigm). Samples were acquired on a Helius mass cytometer (Fluidigm) with a Super Sampler (Victorian Airships, Alamo, Calif) fluidics system. For quality control, the acquisition event rate was maintained at less than 300 events per second. The resulting FCS files were normalized with Calibration Beads, and cell subpopulations were determined by using FlowJo software (FlowJo, Ashland, Ore). Cell events were identified as Ir191/193 double-positive events, and doublets were excluded on the basis of higher DNA content (Ir191) and longer event length. Analysis were performed with FlowJo software and Cytobank (Cytobank, Santa Clara, Calif).

REFERENCES

E1. Weiss ES, Girard-Guyonvarc'h C, Holzinger D, de Jesus AA, Tariq Z, Picarsic J, et al. Interleukin-18 diagnostically distinguishes and pathogenically promotes human and murine macrophage activation syndrome. Blood 2018;131:1442-55.
E2. Poli A, Michel T, Theresine M, Andres E, Hentges F, Zimmer J. CD56bright natural killer (NK) cells: an important NK cell subset. Immunology 2009;126:458-65.
E3. Milush JM, Lopez-Verges S, York VA, Deeks SG, Martin JN, Hecht FM, et al. CD56negCD16(+) NK cells are activated mature NK cells with impaired effector function during HIV-1 infection. Retrovirology 2013;10:158.
E4. Martinelli S, Krumbach OHF, Pantaleoni F, Coppola S, Amin E, Pannone L, et al. Functional dysregulation of CDC42 causes diverse developmental phenotypes. Am J Hum Genet 2018;102:309-20.
E5. Jagadeesh KA, Wenger AM, Berger MJ, Guturu H, Stenson PD, Cooper DN, et al. M-CAP eliminates a majority of variants of uncertain significance in clinical exomes at high sensitivity. Nat Genet 2016;48:1581-6.
E6. Samocha KE, Robinson EB, Sanders SJ, Stevens C, Sabo A, McGrath LM, et al. A framework for the interpretation of de novo mutation in human disease. Nat Genet 2014;46:944-50.

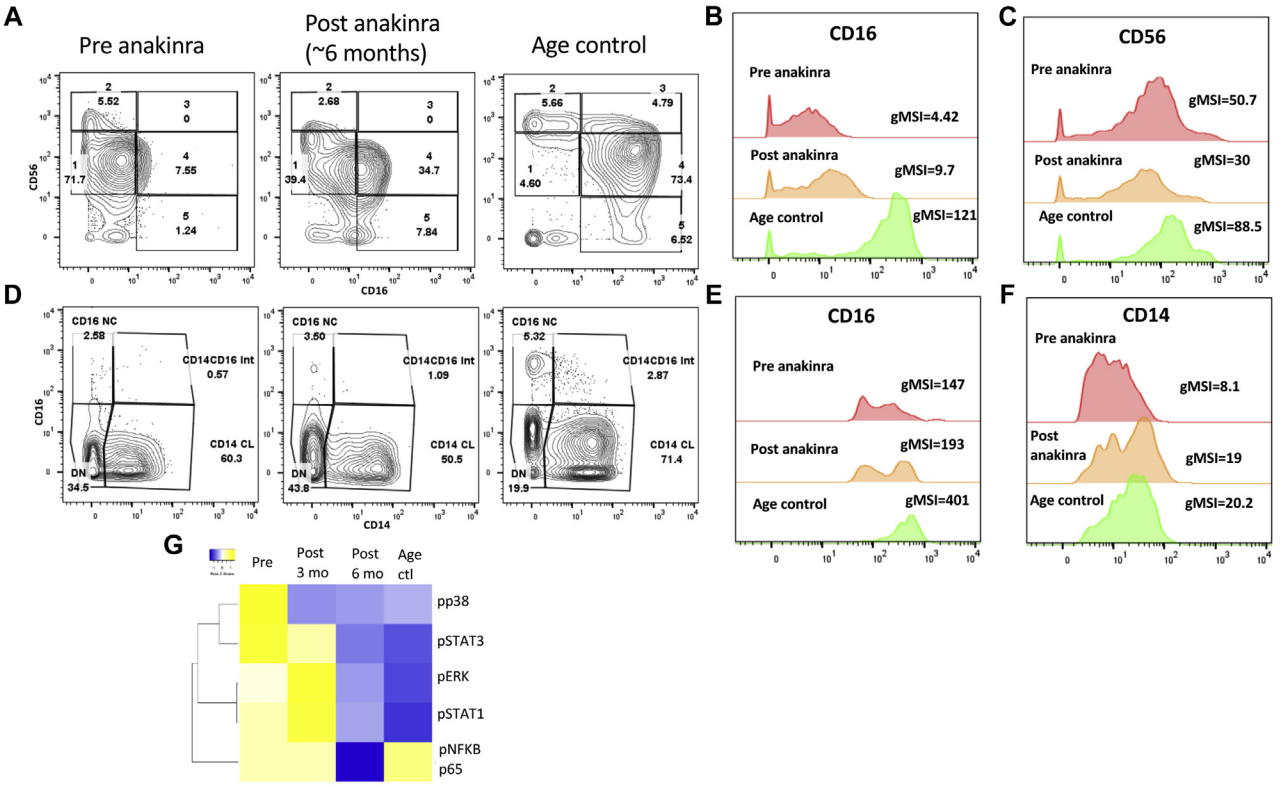

FIG E1. CyTOF analysis of distribution of selected subsets (monocytes and natural killer cells) in PBMCs of patient 1 (for panel, see Table E3). **A,** Low percentage of $CD16^{+}$ monocytes. Two-parameter plots (CD14 × CD16) of monocytes ($CD3^{-}CD19^{-}CD7^{-}$). *CL*, Classical; *DN*, double negative (for CD14 and CD16); *Int*, intermediate; *NC*, Nonclassical. Numbers in quadrants show percentages. **B** and **C,** Low CD16 expression on monocytes. Geometric mean signal intensity *(gMSI)* of CD16 in nonclassical monocytes and of CD14 in classical monocytes. **D,** Decreased percentage of $CD16^{+}CD56^{+}$ natural killer cells, with partial recovery after treatment. Two-parameter plots (CD16 × CD56) of natural killer ($CD7^{+}$) cells are shown. Gates are based on Poli et al[E2]: *1*, $CD56^{+}CD16^{-}$; *2*, $CD56^{bright}CD16^{-}$; *3*, $CD56^{bright}CD16^{+}$; *4*, $CD56^{+}CD16^{+}$; and *5*, $CD56^{-}CD16^{+}$. This subset is observed at low percentages in healthy adults (<5%, Milush et al[E3]). Second-line numbers in quadrants show percentages. **E** and **F,** Low expression of CD16 in total natural killer cells of patient 1. gMSI of CD16 (Fig E1, *E*) and CD56 (Fig E1, *F*) in total natural killer cells. **G,** Decreasing levels of several phosphorylated signaling proteins in CD14 classical monocytes after treatment. A signaling heat map from serial samples, before and after anakinra, based on intracellular levels of phosphorylated proteins is shown. *Age ctl*, Sex-matched pediatric control subject.

TABLE E1. Comparison of the clinical phenotypes and biological parameters of patients with TKS and of our cohort of 4 patients with a *de novo* heterozygous C-terminal mutation in *CDC42*

	TKS			
	Group 1	Group 2	Group 3	C-terminal* mutations in *CDC42*
Clinical presentation				
Failure to thrive, postnatal weight (weight <2 SD)	3/5	2/4	3/4	4/4
Intellectual disability	5/5	4/4	2/6	1/4
Facial dysmorphism, including frontal bossing and large forehead	2/5	2/4	1/6	3/4
Cardiac abnormality	3/5	2/4	2/5	0/4
Rash	0/5	0/4	0/5	4/4
Recurrent severe infections	4/5	3/4	1/6	3/4 (2/3 were receiving immunosuppression)
Biological parameters				
Thrombocytopenia	4/4	1/3	0/5	4/4
Anemia	NA	NA	NA	4/4
Systemic inflammatory syndrome: increased CRP level, ESR, and ferritin level	NA	NA	NA	4/4

Group 1, Switch mutations in *CDC42*; *group 2*, pocket mutations in *CDC42*; *group III*, CRIB mutation as per Martinelli et al;[E4] *NA*, not applicable.
*Affecting the last 3 to 5 amino acids of *CDC42*.

TABLE E2. WES analysis of all 4 reported patients

Patient 1	*CDC42*	c.563G>A	p.C188Y	*De novo*	Possibly pathogenic: 0.337*
Patient 2	*CDC42*	c.563G>A	p.C188Y	*De novo*	Possibly pathogenic: 0.337*
	LYST	c.1686G>C	p.Q562H		Possibly pathogenic: 0.035
	LPIN2	c.446C>T	p.P149L		Possibly pathogenic: 0.049
	MEFV	c.442G>C	p.E148Q		Likely benign: 0.024
Patient 3	*CDC42*	c.556C>T	p.R186C	*De novo*	Possibly pathogenic: 0.053*
	LYST	c.4545G>C	p.E1515D	Heterozygous from father	Likely benign: 0.003
	UNC13D	c.2764G>A	p.A922T	Heterozygous from mother	Possibly pathogenic: 0.047
Patient 4	*CDC42*	c.576A>C (stop lost)	p.*192C*24	*De novo*	Possibly pathogenic: 0.053*
	WAS	c.706G>A	p.A236T	X-linked from mother	Possibly pathogenic: 0.964

*Mendelian clinically applicable pathogenicity scores were used to interpret the pathogenicity of nonsynonymous *CDC42* variants.[E5] The pLI score measures the likelihood that *CDC42* is intolerant to loss-of-function variants; the pLI score for *CDC42* for patients 1, 2, and 3 was 0.79.[E6] As further support for the claims of pathogenicity, these variants are observed in 0 subjects from the gnomAD control population consisting of more than 120,000 presumably healthy subjects (https://www.biorxiv.org/content/10.1101/531210v2).

TABLE E3. CyTOF antibody panel

No.	Label	Target	Clone	μL per sample	Target location	Source
1	89Y	CD45	HI30	0.75	Surface	Fluidigm
2	141Pr	CD235ab (glycophorin)	HIR2	0.1	Surface	Fluidigm
3	142Nd	CD19	HIB19	0.9	Surface	Fluidigm
4	144Nd	CD11b (Mac-1)	ICRF44	0.9	Surface	Fluidigm
5	146Nd	CD64	10.1	0.9	Surface	Fluidigm
6	147Sm	CD11c	Bu15	0.9	Surface	Fluidigm
7	149Sm	CD66a/CEACAM1	CD66a-B1.1	0.9	Surface	Fluidigm
8	150Nd	CD192 (CCR2)	K036C2	0.9	Surface	BioLegend; in-house labeling*
9	151Eu	CD123 (IL-3 receptor)	6H6	0.7	Surface	Fluidigm
10	152Sm	CD36	5271	0.9	Surface	Fluidigm
11	153Eu	CD7	CD7-6B7	0.9	Surface	Fluidigm
12	154Sm	CD163	GHI/61	1	Surface	Fluidigm
13	155Gd	CD45RA	HI100	0.5	Surface	Fluidigm
14	156Gd	p-p38 (T180/Y182)	D3F9	1	Intracellular (phospho)	Fluidigm
15	158Gd	CD33	WM53	0.9	Surface	Fluidigm
16	161Dy	pSTAT1 (S727)	A15158B	1	Intracellular (phospho)	BioLegend; in-house labeling*
17	162Dy	CD80 (B7-1)	2D10.4	1	Surface	Fluidigm
18	163Dy	pSTAT3 (Y705P)	4/pSTAT3	1	Intracellular (phospho)	BioLegend; in-house labeling*
19	164Dy	IκBα	L35A5	1	Intracellular (total protein)	Fluidigm
20	165Ho	CD61	VI-PL2	0.4	Surface	Fluidigm
21	166Er	pNF-κB p65 (S529)	K10-895.12.50	0.5	Intracellular (phospho)	Fluidigm
22	168Er	CD206 (MMR)	15-2	1	Surface	Fluidigm
23	170Er	CD3	UCHT1	0.9	Surface	Fluidigm
24	171Yb	pERK 1/2 (T202/Y204)	D13.14.4E	1	Intracellular (phospho)	BioLegend; in-house labeling*
25	172Yb	CX3CR1	2A9-1	1	Surface	Fluidigm
26	173Yb	Iba1	ab5076	1	Intracellular (total protein)	Abcam; In-house labeling*
27	174Yb	HLA-DR	L243	0.9	Surface	Fluidigm
28	175Lu	CD14	M5E2	1	Surface	Fluidigm
29	176Yb	CD56 (NCAM)	NCAM16.2	0.9	Surface	Fluidigm
30	209Bi	CD16	3G8	0.9	Surface	Fluidigm

CEACAM1, Carcinoembryonic antigen related cell adhesion molecule 1; *IL-3R*, IL-3 receptor; *MMR*, macrophage mannose receptor; *NCAM*, neural cell adhesion molecule 1; p*NF-κB*, nuclear factor κB; *pERK*, phosphorylated extracellular signal-regulated kinase; *pSTAT*, phosphorylated signal transducer and activator of transcription.
*Labeled by using the Maxpar X8 Antibody Labeling Kit (Fluidigm).